View metadata, citation and similar papers at core.ac.uk

brought to you by CORE

provided by IntechOpen

We are IntechOpen,
the world's leading publisher of
Open Access books
Built by scientists, for scientists

4,800
Open access books available

122,000
International authors and editors

135M
Downloads

154
Countries delivered to

Our authors are among the
TOP 1%
most cited scientists

12.2%
Contributors from top 500 universities

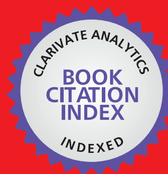

WEB OF SCIENCE™

Selection of our books indexed in the Book Citation Index
in Web of Science™ Core Collection (BKCI)

Interested in publishing with us?
Contact book.department@intechopen.com

Numbers displayed above are based on latest data collected.
For more information visit www.intechopen.com

Chapter

Nanoscale Optical Patterning of Amorphous Silicon Carbide for High-Density Data Archiving

Tania Tsvetkova

Abstract

The work presented here is related to some developments in providing a new generation ultrastable (>100 years), ultrahigh density (>1 Tbit/sq.in.) data storage materials for archival applications. The chosen material to write nanoscale data by finely focused ion beams is hydrogenated amorphous silicon carbide (a-SiC:H) films. Wide bandgap a-SiC:H has been chosen for its appropriate optical, chemical and mechanical properties. Ga^+ was prefered as the implant species for the focused ion beam (FIB) implantation due to its widespread uses in FIB equipment and its modifying effects on the amorphous silicon carbide target. A range of a-SiC:H film samples have been FIB patterned under different implantation conditions for this study. The emphasis in these investigations was the influence of different substrate temperatures on the patterning process. The effects of further annealing of room temperature implanted samples were also studied. The FIB patterned samples under different conditions were analysed using near-field techniques, like atomic force microscopy (AFM), to define optimum implantation parameters for archival data storage applications. Using the established optimal conditions for the FIB patterning process of a-SiC:H films, it is expected to achieve the aimed ultrahigh density and stability with this novel data storage method for archival applications.

Keywords: optical data storage, nanoscale data archiving, focused ion beams

1. Introduction

The archival sector is becoming increasingly important, due in part to the introduction of new legal requirements governing the storage of governmental and commercial data but also as a consequence of the ever-increasing amount of digital data generated by all aspects of our everyday life. Indeed, it has been estimated [1] that the total archival capacity required worldwide is expected to exceed 1000 exabytes by 2020, generating market values of in excess of $50 billion. For archival applications reliability, data integrity and media longevity feature much more prominently than in other storage sectors. The main recognized archival storage media currently in use are magnetic tape and optical disks, although it is estimated that around 50% of the archive data for commercial organizations is in fact held on magnetic hard disk drives [2]. While optical disks for professional archiving are usually 'guaranteed' a lifetime of at least 50 years, magnetic tapes and disks have in general a much shorter predicted lifespan. The lifetime of magnetic hard disk media in particular is reducing as the storage density increases due to the superparamagnetic effect, with lifetimes of current

high-capacity drives limited to around 10 years. Magnetic tape, while a very good choice for high-capacity short-term storage such as backup and disaster recovery, is yet rather delicate contact media, which can become physically damaged with use, and so can degrade with time, while also the magnetic data can be easily lost when exposed to magnetic fields. Hence, to retain tape data available over extended periods of time, tapes must be frequently re-tensioned and data be periodically refreshed (read and rewritten)—a potentially complex and costly task with serious consequences if not managed properly. It is clear therefore that archival storage is an exceedingly important application and it is equally clear that conventional archival storage media are quite limited in terms of lifetime and, particularly for optical disks and magnetic tapes, in terms of storage density (bits per square inch). It is in this context that the present work has aimed to develop novel, ultra-stable and ultrahigh density storage media for archival applications. Indeed, the approach of ion implantation in SiC can potentially lead to extremely long (many hundreds of years) data lifetimes, which may find application in the long-term preservation of important scientific and cultural assets.

2. Nanoscale optical patterning of amorphous silicon carbide films by Ga^+-focused ion implantation

To realize our goal of 'permanent' high-density storage, we have chosen amorphous hydrogenated silicon carbide (a-SiC:H) as a storage medium. a-SiC:H is an exciting material with a wide range of useful optical and electrical properties (e.g., high transparency in the visible region due to its wide optical band gap from 1.8 to 3.0 eV), as well as mechanical durability and chemical inertness [3]. These properties, together with ease of fabrication and a remarkable thermal stability, make SiC a very promising candidate for various optoelectronic, photonic and other device applications (e.g., solar cells, light-emitting diodes, imaging sensors, high-power microwave devices, high-energy radiation detectors), particularly in adverse environments [3, 4]. The relative immunity of SiC to environmentally induced degradation, in particular its high thermal stability (stable to temperatures in excess of 1500°C), makes it attractive for data storage applications, and promising results have been achieved by using ion implantation to write micro- and nanoscale marks in SiC films [5–11].

Ion-beam implantation is a standard technique for controlling electrical, band gap and optical properties of semiconductors (see, e.g., [12]), and some data exist for the SiC materials. Recently the ion-beam implantation route has attracted renewed interest due to the development of computer-controlled focused-ion-beam systems that enable the fabrication of sophisticated ion-implanted structures [11, 13, 14]. The focused-ion-beam diameter can be <10 nm, allowing the modification of the dielectric and optical properties of materials on this same nanoscale (10 nm bit sizes is roughly equivalent to a data density of 10 Tbit/sq.in.). Such nanoscale property changes in optical transmission and reflection offer ultrahigh density yet permanent optical data archives. To readout such high-density optical data, a super-resolution (sub-diffraction) optical technique is required. In the laboratory environment and for research purposes, this can be provided by scanning near-field optical microscopy (SNOM) [15]. SNOM techniques have been successfully applied for studies of ion-beam modifications in silicon carbide in infrared [16] and visible [8] spectral ranges. Of course imaging by SNOM is slow (and expensive), but for practical applications, other super-resolution readout techniques, such as the use of solid-immersion lens (SIL) optics [17], the so-called super-RENS technique [18] or arrays of scanning near-field apertures, might ultimately be used to achieve the necessary readout data rates (and required system cost).

2.1 Ga^+ ion beam-induced optical contrast in amorphous silicon carbide

Several ion-implanted species have already been investigated for the modification of the optical properties of a-SiC:H thin films, including Ar^+, ions of group IV elements [5, 7–9] and, most recently, Ga^+. The use of gallium is attractive since it is available in standard FIB machines and in addition has been shown to be capable of generating large optical contrasts [6]. Investigations were carried out further in order to study the structural and chemical bonding modifications of thin a-SiC:H films when using high-dose Ga^+ ion implantation, resulting in considerable changes of the optical band gap and the electronic properties of the material [6, 7].

The Ga^+ ion implantation has yielded in a considerable optical effect as registered by the results of transmission, reflection and PDS measurements, used further to derive the absorption coefficient spectra, shown in **Figure 1**. This effect becomes more markedly pronounced as the dose increases. As seen from the figure, the optical absorption edge moves to lower photon energies while also being accompanied by an increase of the absorption coefficient in the measured energy range, as a result of the Ga^+ ion implantation.

The optical absorption edge shift increases with the ion dose, signifying a corresponding change in the density of states distribution in the optical gap. It could be assumed, therefore, that the observed changes are related to the breaking of bonds due to ion bombardment and modification of the chemical bonding arrangements of the host atoms due to the presence of the implanted Ga^+ ions. This assumption is also supported by the registered changes in the absorption spectra in the IR region shown in **Figures 2** and **3**. The well-defined peak at about 2080 cm^{-1}, related to the stretching vibration mode of Si-H bonds in a-SiC:H films for the non-implanted case, shows well-expressed tendency to decrease. Notably, it is also shifting towards lower energies with the increase of the ion dose (**Figure 2**).

This shift could be attributed to an underlying mechanism of interaction between the ions of the added element with the Si atoms in the host material, resulting in a change of the Si-H stretching mode. This behaviour could be explained remembering the lower electronegativity of the implanted Ga atoms than the C host atoms in the target material, so that Ga will be substituting for the C atom in the C-Si-H bond, as in the previously reported case of Ge and Sn ion implantation in a-SiC:H films [19–21]. The observed accompanying decrease of the peak with the ion dose is further confirmed for the modifying effect of the Ga ion bombardment on the bonding configuration of the host atoms and is an evidence for the breaking of the Si-H bonds which is accompanied by considerable loss of hydrogen.

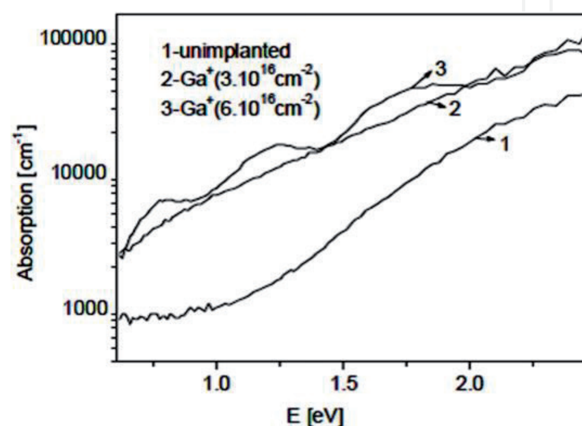

Figure 1.
Optical absorption coefficient α of a-$Si_{0.85}C_{0.15}$:H films: unimplanted (1) and Ga^+ implanted at doses (in cm^{-2}) 3×10^{16} (2) and 6×10^{16} (3) [7].

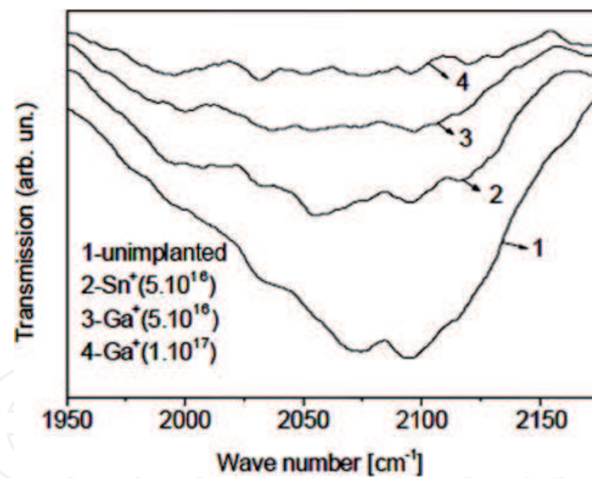

Figure 2.
IR transmission spectra in the region 1950–2200 cm^{-1} of an unimplanted a-$Si_{0.85}C_{0.15}$:H film (1) and a-$Si_{0.85}C_{0.15}$:H films implanted with Sn^+ at dose D = 5 × 10^{16} cm^{-2} (2) and Ga^+ with doses D = 5 × 10^{16} cm^{-2} (3) and D = 1 × 10^{17} cm^{-2} (4) [7].

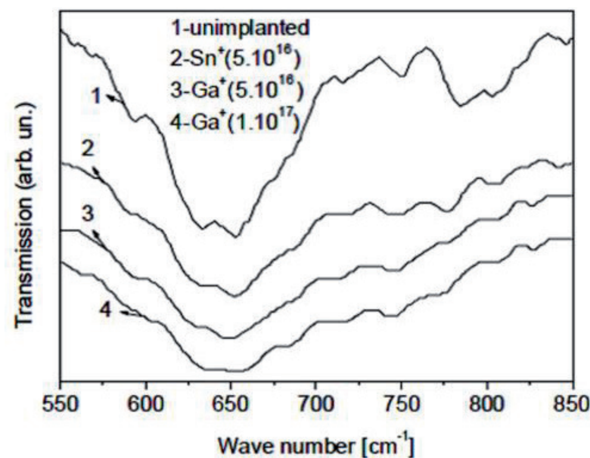

Figure 3.
IR transmission spectra in the region 550–850 cm^{-1} of an unimplanted a-$Si_{0.85}C_{0.15}$:H film (1) and a-$Si_{0.85}C_{0.15}$:H films implanted with Sn^+ at dose D = 5 × 10^{16} cm^{-2} (2) and Ga^+ with doses D = 5 × 10^{16} cm^{-2} (3) and D = 1 × 10^{17} cm^{-2} (4) [7].

As also demonstrated in **Figure 2**, the modification effect of Ga^+ ion implantation on the bonding configurations of the host atoms in the a-SiC:H films is very similar to the one of Sn^+ ion implantation in a-SiC:H films [22]. Apparently, less explicit but still observable are the changes in the region 550–800 cm^{-1} shown in **Figure 3**. In the same figure, the observed change of the Si-C bond stretching mode as shown at ~780 cm^{-1} [23, 24] signifies the modification of the Si-C bonding arrangements in the a-SiC:H host material, the mechanism including considerable Si-C bond breaking as a result of the Ga^+ ion bombardment.

The Raman measurement results presented in **Figure 4** could also be considered as confirmation of the above reasoning. Again in this case, there is a registered well-expressed effect of increased disordering of the silicon network, similar to the earlier results of Sn^+ ion implantation in a-SiC:H films [22]. Here this is demonstrated in the figure by a considerable decrease of the Si-Si bond related peak in the spectra near 500 cm^{-1}.

The investigation results presented here for the case of Ga^+ broad-beam implanted a-SiC:H films have shown various structural and chemical modification changes, resulting in an effective optical bandgap decrease. The underlying mechanism of these modifications comprises breaking of Si-H and C-H bonds

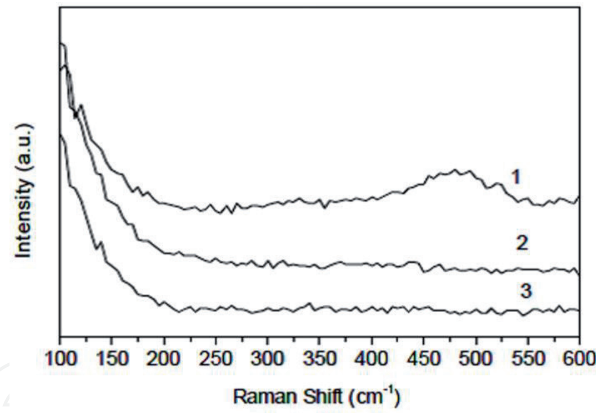

Figure 4.
Raman spectra of an unimplanted a-$Si_{0.85}C_{0.15}$:H film: (1) and a-$Si_{0.85}C_{0.15}$:H films implanted with Sn^+ (2) and Ga^+ (3) at a dose $D = 5 \times 10^{16}$ cm^{-2} [7].

and accompanying considerable loss of H in the target material as a result of the ion bombardment. The IR and Raman investigations also reveal increased Si-C bond breaking and formation of Si-Ga bonds, bearing in mind the lower electronegativity of the implanted Ga atoms, compared with the C host atoms, and assuming Ga will substitute for the C atom in the C-Si-H bond [5, 7]. Yet, due to the very low melting point (T_m = 29.8°C) of Ga, some part of the implanted Ga ions are inevitably embedded as Ga clusters and are not directly bonded chemically to the host atoms [25].

2.2 Ga^+-focused ion beam patterning of amorphous silicon carbide

The particular attention that has been focused on Ga^+ as the implant species is due to the fact of its widespread use in FIB systems. Computer-generated Ga^+ FIB pattern in an a-SiC:H film is demonstrated in **Figure 5** [6]. The figure represents an optical micrograph of an a-SiC:H thin film with a variety of Ga^+ FIB-created patterns. The combined pattern consists of a number of chess-board-like (CBL) and series-of-line (SL) patterns, implanted with different doses. The optical density of the irradiated areas is increased, due to ion bombardment, as a result of which they are seen as optically darker regions in the picture.

The computer-generated FIB-irradiated pattern, presented in the figure, comprises several patterns of line series and chess-board-type fields with varying sizes and doses of implanted Ga^+. In this picture, the shorter line series patterns LS1 (size 2.5/2.5/20 μm) and the longer line series patterns LS2 (size 5/5/40 μm) were FIB written with Ga^+ ion doses in the range $D = 5 \times 10^{15} \div 2 \times 10^{17}$ cm^{-2}. The big chess-board-type field (BCF) (size 20 μm) and the smaller chess-board-type fields SCF1 and SCF2 (both size 10 μm) were made with Ga^+ ion doses $D_1 = 2.5 \times 10^{16}$ cm^{-2} (BCF and SCF1) and $D_2 = 4 \times 10^{16}$ cm^{-2} (SCF2). The picture shows the potential of this method for applications in high-density optical data storage, as well as for direct writing of submicron lithographic masks for further uses in micro- and optoelectronics.

3. Near-field analysis of FIB-patterned amorphous silicon carbide

Near-field techniques were used for the study of the FIB-patterned amorphous silicon carbide films. The topography of the FIB-patterned samples was analysed with an atomic force microscope (dimension 3000 digital instruments). Scanning near-field optical microscope was employed to study and compare the changes in

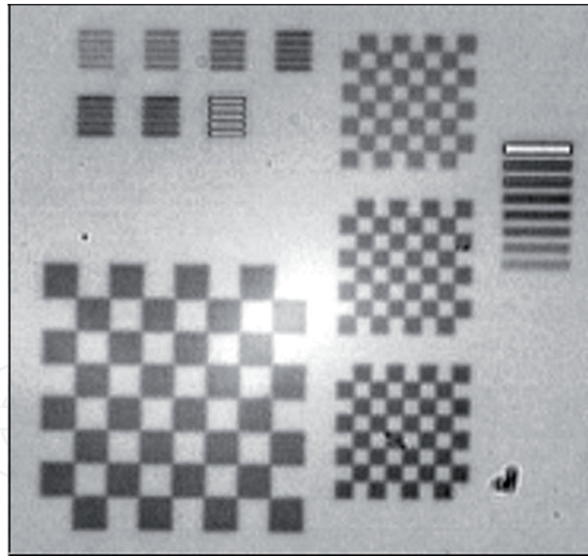

Figure 5.
Micron-scale combined pattern on an a-SiC:H film written with a FIB system by using a 15 pA Ga^+-focused ion beam. The size of the big chess field is 20 × 20 μm² [6].

the local optical absorption of the irradiated (patterned by design) areas relative to the nonirradiated ones.

3.1 Atomic force microscopy (AFM) studies of FIB-patterned a-SiC:H

Before proceeding with the SNOM experiments, topographic images of the FIB-patterned areas were recorded and studied with AFM [8]. The AFM results are presented in **Figure 6** for the CBL and SL structures, and apparently the irradiated areas are topographically lower than nonirradiated ones. Presumably this is due to the ablation of the thin film caused by the ion irradiation. A cross-sectional view of the AFM image of a SL is shown in **Figure 6b**. The ion dose is highest for the left-hand side (3.2×10^{16} cm^{-2}), and it is decreasing towards the right-hand side (0.8×10^{15} cm^{-2}) of the SL pattern. These results suggest that the higher ion doses cause larger topography variations, which should be expected.

Further important result observed in **Figure 6b** is that each line of the SL pattern is as large as ~11 μm, even though the beam diameter of the Ga^+ ion beam was set to be ~50 nm. This unexpectedly large line width of the SL pattern is probably the result of imperfect charge neutralization which leads to severe charge buildup, causing distortion and defocusing of the Ga^+ ion beam during the irradiation.

3.2 Scanning near-field optical microscopy analysis of FIB-patterned amorphous silicon carbide

The implanted set of patterns was characterized by SNOM measurements using a custom-built microscope. The details of the SNOM measurements are described elsewhere [8, 9]. In short, an unpolarized beam from a He-Ne laser (633 nm) is scanned over the substrate side of the sample. The laser beam is kept defocused keeping the laser intensity over the scanned area as uniform as possible. The light passing through the patterned area is then collected using a sharp, uncoated optical fibre probe from one point to another for mapping the optical images obtained by the near-field method. The gap between the probe end and the sample surface is kept

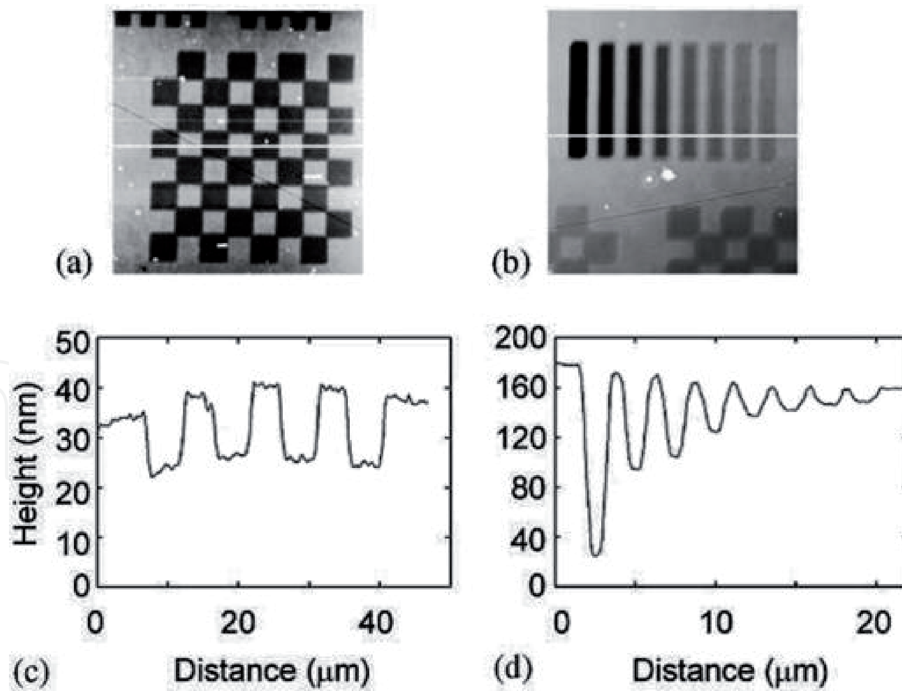

Figure 6.
AFM images of CBS (a) and SSL (b) patterns written in an a-SiC:H film with Ga^+ FIB. The cross-sections indicated in (a) and (b) are shown in (c) and (d), respectively [8].

constant by non-optical shear-force technique and the feedback from the shear-force regulation scheme, providing the required topographic information. Thus, topography mapping and local optical mapping are both registered simultaneously.

The SNOM experiments can provide an optical image of the corresponding topographic image simultaneously, as already mentioned. A series of CBL patterns with different doses have been investigated with SNOM in order to demonstrate its potential. The obtained topographic and corresponding optical images with SNOM are represented in **Figure 7**. When compared with unpatterned areas, e.g., in the left-hand side of the image or in some parts of the CBS pattern, the areas irradiated with ion beam are topographically lower, while they appear also optically darker in the SNOM image. The observed trend of the topographic features of the irradiated

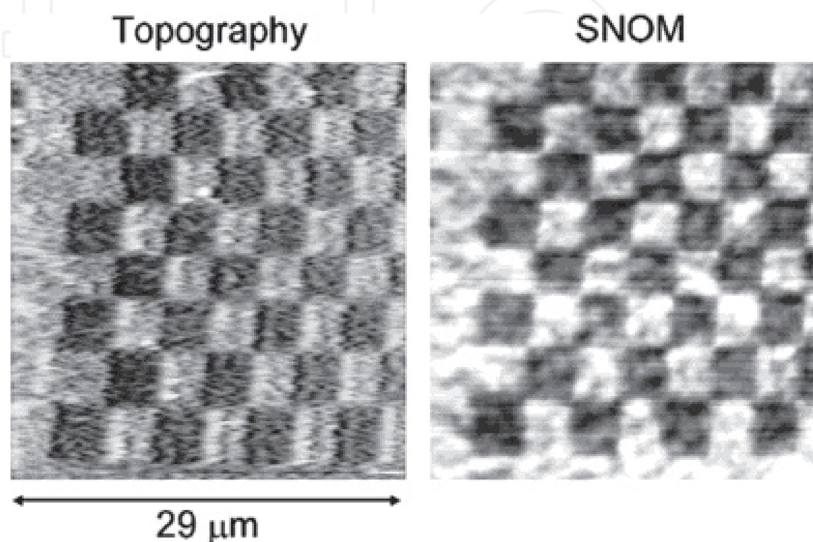

Figure 7.
Topographic image (left) and corresponding SNOM image (right) of a CBS pattern created on an a-SiC:H thin film by irradiation with Ga^+-focused ion beam [8].

areas appears to be the same as that obtained with the AFM. The trend of the optical contrasts observed with SNOM is qualitatively the same as the one obtained in the conventional optical microscopy case (e.g., see **Figure 5**).

4. Ion-implantation temperature and post-implantation annealing effects on the ion beam-induced optical patterning of a-SiC:H

Gallium has also previously been used to make both embedded thin films and layers rich in Ga nanoparticles for broadband high reflectivity devices (such as sunglasses). For the interpretation of these earlier studies in optical glasses, the reflectivity control by the Ga implantation was linked to the fact that Ga has a very low melting point (T_m = 29.8°C) and a rather unusual feature of volume contraction upon melting. These factors were assumed to contribute to Ga incorporation as dispersed clusters and/or small nanoparticles [26, 27]. There was also preferential diffusion and loss of Ga from the implanted region. Any such changes not only influence the implant zone but in turn can modify the interzone reference regions both from changes in the H content, lateral in-diffusion of Ga and induced stress due to the volume changes associated with gallium nanoparticles. Such changes are very sensitive to the implant temperature. It was noted that Ga precipitation into nanoparticles can vary dramatically (in terms of particle size) with concentration and small changes in surface implant temperature [28]. Overall, these factors will contribute to the maximum optical contrast (readout signal) between implanted and unimplanted regions and will also play a significant role in determining the lifetime of the recorded information.

The precise role of implantation temperature effects of target temperature during Ga^+ ion irradiation on the forms of Ga incorporation in the SiC:H film, and hence on the optical contrast obtainable, has therefore formed a key part of this research. This could allow optimization of the process not only from the point of view of the implantation itself (i.e., maximize processing speed and minimize implant costs) but also from the point of view of data storage density, readout contrast and data longevity. Experience also suggests that appropriate post-implantation annealing treatments could offer further benefits in reducing the required ion dose [29] and enhancing contrast, thus increasing the cost-effectiveness of the FIB bit-writing method. Hence, we have also investigated a range of post-implantation treatments in order to determine the most appropriate route for dose reduction while maintaining suitable readout contrast.

4.1 Investigation of the thermal effects on the Ga^+ ion beam-induced optical contrast and structural modification of amorphous silicon carbide

The effects of implantation temperature and post-implantation thermal annealing on the Ga^+ ion beam-induced optical contrast formation in hydrogenated silicon-carbon alloy films have been further studied [30, 31]. For these studies, Ga^+ broad-beam ion implantation in a-SiC:H samples was chosen to be carried out at different film substrate temperatures (T_1 = RT (room temperature), T_2 = LN_2 (liquid nitrogen) and T_3 = +50°C). Then some of the RT implanted samples were thermally annealed post-implantation at higher temperatures. The benefits expected for the optical data storage method, relying on a readout of reduced optical transmission as detected by SNOM [15, 26], were as follows: (1) lower implantation temperature should result in an increased amount of defects which will be leading to an absorption increase, i.e., further decrease in transmission (hence greater readout contrast); (2) higher implantation temperatures, or high-temperature post-implantation annealing, were expected to lead to a possible increase in the optical

reflectivity and hence decrease in transmission, due to Ga clusters coalescing into bigger light-reflecting Ga colloid particles.

A range of in a-SiC:H samples have been implanted with Ga^+ broad-beam ion implantation at different substrate temperatures (from liquid nitrogen (LN_2) temperatures to around room temperature (RT) and also at a higher temperature T = +50°C). Some of the RT implanted samples were further post-implantation thermally annealed at several different temperatures in vacuum. The whole range of implanted and annealed samples were optically studied, using optical transmission spectroscopy in the UV–VIS range, in order to define the optimum implantation conditions for archival data storage applications. Using the established optimal dose, $D = 2D_3 = 5 \times 10^{16}$ cm^{-2} [30], the transmission (T), the reflection (R) and the absorption coefficient α of Ga^+ implanted a-$Si_{1-x}C_x$:H ($x_1 = 0.18$) films at different temperatures (T_1 = RT, T_2 = LN_2 (liquid nitrogen) and T_3 = +50°C) were studied (**Figure 8**).

For further post-implantation annealing studies, some of the RT implanted a-$Si_{1-x}C_x$:H ($x_1 = 0.18$) samples were annealed at higher temperatures (T_1 = +50°C, T_2 = +120°C and T_3 = +250°C) and optically characterized by measurements of the transmission T, the reflection R and the absorption α (**Figure 9**). The obtained results do not represent any appreciable transmission change, even for the higher dose $D = 2D_3 = 5 \times 10^{16}$ cm^{-2} and for the highest annealing temperature T_3 = +250°C. Even though in this case there is some slight increase in reflectivity detected, compared to the RT implanted sample, the ion beam-induced thermal annealing of the irradiation defects, which results in absorption decrease, compensates this effect, resulting in similar transmission change as the one for the RT implantation case.

The presented results have indicated the optimum conditions for the new optical data recording method which uses the reading near-field technique SNOM, chosen to be working in optical transmission mode. The results demonstrate that the greatest effect on the optical transmission T is achieved for the RT implanted samples. In the lower temperatures case, the expected ion beam-induced increased defect introduction, resulting in absorption α increase, does occur. However, the simultaneous ion beam-induced thickness decrease due to sputtering compensates this effect, resulting in lower transmission change than the RT implantation case. Likewise, Ga^+ implantation at increased temperatures does result in increased reflectivity R of the implanted films, presumably due to Ga^+ nanoscale particles coalescing into bigger, light-reflecting clusters. Yet, the simultaneously occurring thermal annealing of the ion beam-induced radiation defects in the films decreases the absorption α, resulting in a lower transmission change than the RT implantation case.

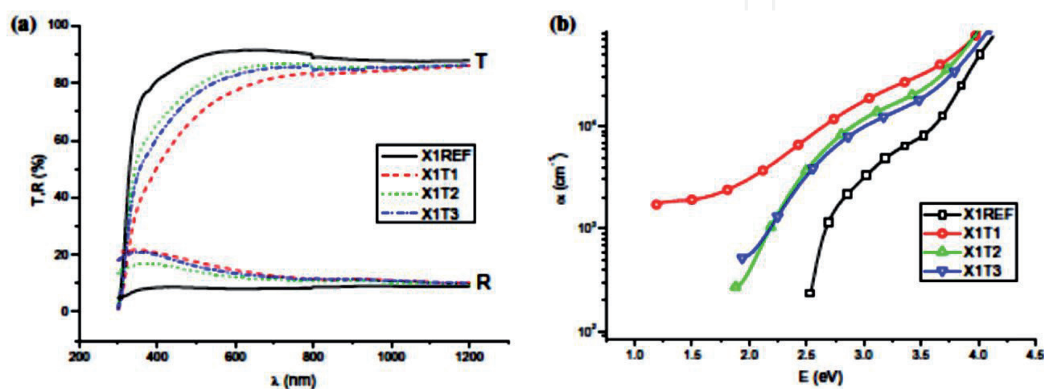

Figure 8.
Transmission (T) and reflection (R) (a), and absorption coefficient α (b), of Ga^+-implanted a-$Si_{1-x}C_x$:H ($x_1 = 0.18$) films with a dose $D = 2D_3 = 5 \times 10^{16}$ cm^{-2}, at different temperatures: T_1 = RT (room temperature), T_2 = LN_2 (liquid nitrogen) and T_3 = +50°C [30].

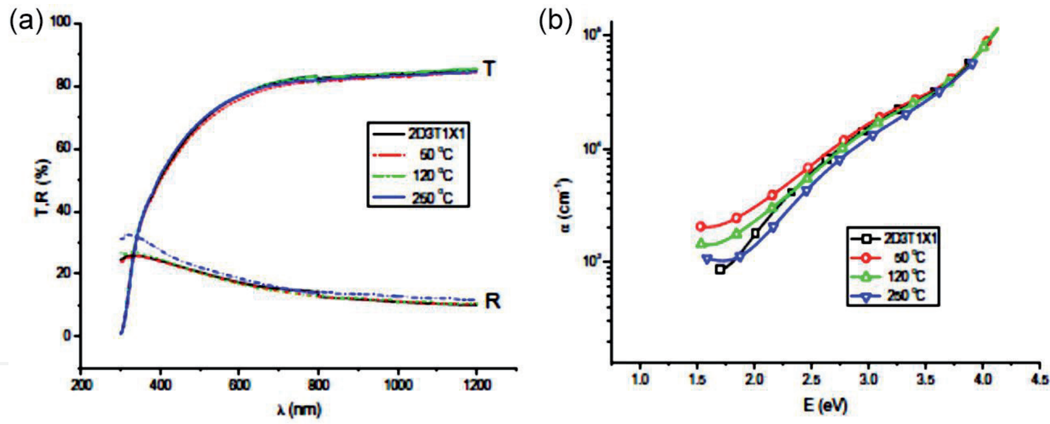

Figure 9.
Transmission (T) and reflection (R) (a) and absorption coefficient α (b), of Ga^+ implanted a-$Si_{1-x}C_x$:H (x_1 = 0.18) films with dose $D = 2D_3 = 5 \times 10^{16}$ cm^{-2} at RT and then annealed at different temperatures: T_1 = +50°C, T_2 = +120°C and T_3 = +250°C [30].

Summarizing, studying the effects of implantation temperature and post-implantation thermal annealing on the Ga^+ ion beam-induced optical contrast formation in hydrogenated silicon-carbon alloy films has led to some practical conclusions [30]. The reasoning about the benefit of lower implantation temperature for the new optical data storage method, relying for optical data readout on reduced optical transmission as detected by SNOM working in transmission mode, was that a lower implantation temperature would lead to an increased amount of introduced defects resulting in an absorption increase, i.e., further decrease in transmission (hence greater data readout contrast). The expected effect was indeed registered but was apparently overridden by an effect of increased ion beam-induced sputtering, which greatly reduced the film thickness and thus increased the transmission in the irradiated films. These results are consistent with those in the case of the Ga^+ FIB patterning of a-SiC:H films, where an increase of both the depth and the width of the individual line patterns within the combined written patterns at the lower temperature case has also been observed as a result of an increased ion beam-induced sputtering [32].

On the other hand, the expected advantage of higher implantation temperatures, or high-temperature post-implantation annealing processing, was that in both cases, the higher temperatures would lead to an increase in the optical reflectivity and hence decrease in transmission, due to Ga clusters effectively coalescing into bigger, optically reflecting Ga colloid particles, resulting in a higher readout contrast. The predicted effect of optical reflectivity increase was indeed observed but was overridden in this case by an apparent decrease in absorption (hence increase in transmission), both in the high-temperature implanted or annealed samples, due to a decrease in the ion beam-introduced defect concentration, as a result of thermally enhanced self-annealing. Thus, it can be concluded that the best conditions for optical data storage for archival storage applications when using Ga^+ ion implantation in a-SiC:H films were found to be at room temperatures with an optimal dose. The conclusion that the optimum implantation temperature for storage applications has to be that of room temperature appears advantageous since it means that the required ion-implantation process can be simplified and reduced in cost.

4.2 Ion-implantation temperature effects on the nanoscale optical patterning of amorphous silicon carbide by Ga^+-focused ion beams

Focused Ga^+ FIB ion implantation was used to write nanoscale data into hydrogenated amorphous silicon carbide films. As was previously reported,

Ga precipitation into nanoparticles can vary greatly (in terms of the particle sizes) with Ga concentration and small variations in the sample surface temperature [25]. Therefore, the precise role of the effects of the implantation temperature, i.e., the target surface temperature during Ga^+ ion implantation and appropriate post-implantation annealing treatments of the FIB-patterned samples at different temperatures, were studied with respect to optical contrast achieved [30] and obtained data storage densities/feature size (present chapter section) [32], in order to further optimize the cost-effectiveness of the FIB bit-writing method for data archiving.

For this purpose, a range of wide bandgap a-SiC:H thin film samples has been prepared by Ga^+-focused ion beam patterning [32]. The samples have been FIB-patterned under different implantation conditions, with emphasis on the different substrate temperatures (from 0°C temperature to around room temperature). Some of the RT implanted samples were further annealed at +250°C in vacuum. The FIB-patterned samples were then analysed using near-field techniques, like atomic force microscopy, to define the optimum implantation conditions and their implications for archival data storage applications.

Focused Ga^+ implantation in these samples was performed with the FIB system simultaneously employing a charge neutralizer (electron-beam shower) to implant a series of FIB patterns with different ion doses in the range 1×10^{15}–1.25×10^{17} ions cm^{-2}. This choice of the Ga^+ ion doses range has been prompted by our earlier Ga^+ broad-beam implantation results, where the optimized range of ion doses for Ga^+ and other elements has been established to be the same so to yield an optimal optical contrast. The chosen type of the combined implanted FIB pattern for this experiment consisted of combination of four individual patterns: a full square, an open square and two sets of parallel lines. They were situated around a central cross-feature (designed for an eye-guide in the AFM microscope to help finding the area of the nanoscale pattern at the start of each measurement) (**Figure 10**).

In these measurements atomic force microscope (AFM), type Dimension 3000 Digital Instruments [8, 9], was used to analyse the topography of the designed FIB-patterned samples. A lab-built scanning near-field optical microscope [8, 9, 15] was also employed to study the sample morphology and the existing film non-homogeneities in the as-deposited a-SiC:H films.

Initially, the as-deposited and some broad-beam Ga^+ implanted samples were analysed with high-resolution optical imaging using SNOM. The AFM imaging was carried out with a range of different wavelengths (λ = 500÷800 nm), including the wavelength of the He-Ne laser used for the further SNOM analysis of the FIB-patterned samples (λ = 633 nm).

The obtained results showed that both the as-deposited and the ion-implanted samples exhibit sub-μm scale nonuniformities, with regions of lower and higher optical absorptions, presumably due to variations in the samples stoichiometry at the sub-μm scale. The SNOM image of these nonuniformities is shown in **Figure 11** for the case of the a-$Si_{1-x}C_x$:H (x_2 = 0.35) sample implanted with Ga^+ with a dose $D = 5 \times 10^{16}$ cm^{-2}.

The preliminary designed actual patterns consisted of a combination of the above described individual patterns, each of which was ion implanted at four different Ga^+ ion doses: 1×10^{15}, 5×10^{15}, 2.5×10^{16} and 1.25×10^{17} cm^{-2}. For creating these patterns, a specially designed programme was used with the Ga^+ FIB equipment. The length of the individual lines in each pattern, as well as the side of the full and open-squares pattern, was chosen to be 5 μm, while all line widths were fixed to be 200 nm.

While some low temperature (0°C) implanted samples were prepared, a greater number of RT implanted samples were designed with view of the planned following post-implantation annealing treatments for the investigation of their effect on

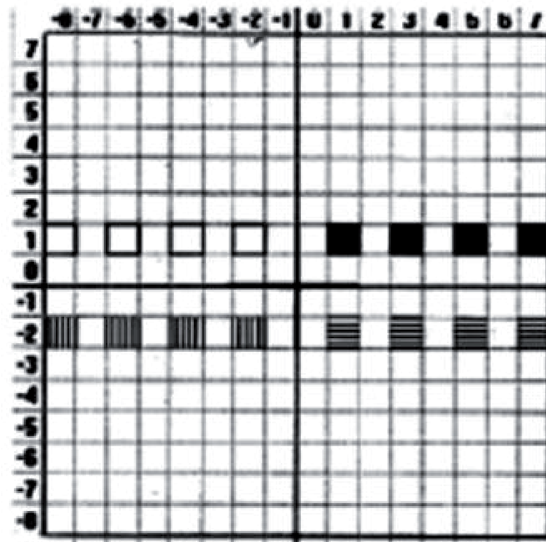

Figure 10.
Combined FIB pattern consisting of individual square patterns [32].

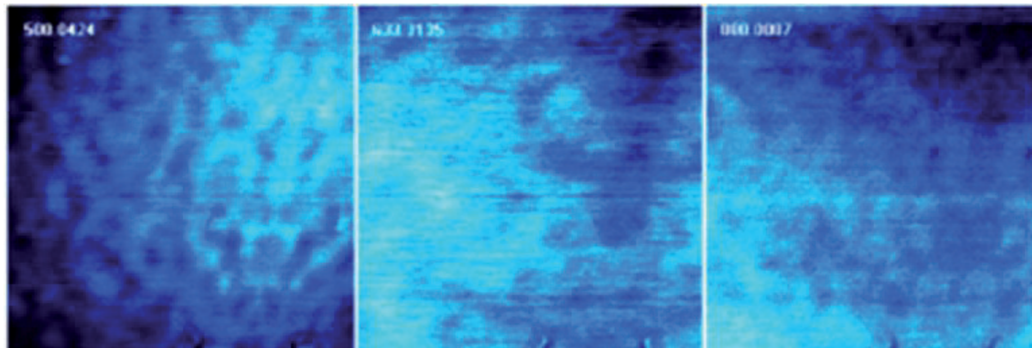

Figure 11.
Images of high-resolution SNOM optical mapping (25 × 25 μm^2) of an a-$Si_{1-x}C_x$:H (x_2 = 0.35) sample broad-beam ion implanted with Ga^+ with a dose D = 5 × 10^{16} cm^{-2} [32].

the recorded optical pattern characteristics, to be further studied using near-field techniques (AFM).

The AFM topographic analysis of the FIB-patterned samples has been focused mainly on the open-square patterns (example shown in **Figure 12**). The AFM results for RT and 0°C implanted samples revealed an increased ion beam-induced sputtering yield for the 0°C implanted samples as compared to the RT implanted ones, similarly to the results in the Ga^+ broad-beam implantation studies. Here, in the Ga^+ FIB case, this resulted in an increase of both the depth and the width of the individual lines within the FIB patterns (see **Table 1**).

For studying the post-implantation annealing effects, some of the RT Ga^+ FIB-implanted a-$Si_{1-x}C_x$:H samples have been thermally annealed in vacuum at T = 250°C. The investigations with AFM topographic analysis of the RT FIB-implanted and the thermally annealed samples have been focused again on the open-square patterns (**Figure 13**, showing the examples for the highest doses in the a-$Si_{0.65}C_{0.35}$:H samples).

The presented AFM results for the RT implanted and the thermally annealed samples revealed slight changes in the depth of the individual lines within the FIB written patterns with the annealing. There is a noticeable decrease of the depth of the individual lines after thermal annealing, denoting slight thickness increase in the irradiated areas of the films, which should contribute to their increased optical absorption and hence result in an increased optical contrast as compared to the

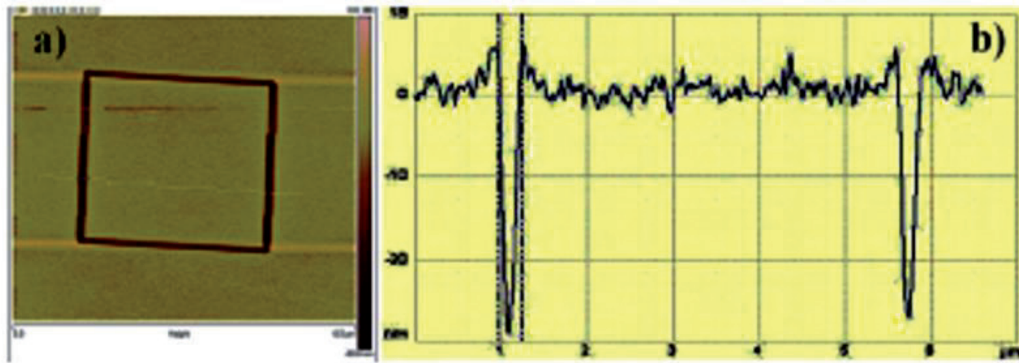

Figure 12.
AFM topographic image (a) and corresponding cross-section (b) of a FIB written open-square pattern in an a-$Si_{1-x}C_x$:H (x_2 = 0.35) sample with a Ga^+ ion dose D = 1.25 10^{17} cm^{-2} [32].

a-$Si_{1-x}C_x$:H		$D_1 = 1 \times 10^{15}$ cm^{-2}		$D_2 = 5 \times 10^{15}$ cm^{-2}		$D_3 = 2.5 \times 10^{16}$ cm^{-2}		$D_4 = 1.25 \times 10^{17}$ cm^{-2}	
		h_1 [nm]	w_1 [μm]	h_2 [nm]	w_2 [μm]	h_3 [nm]	w_3 [μm]	h_4 [nm]	w_4 [μm]
$x_1 = 0.18$	RT	3	0.25	4	0.30	4	0.70	4.5	0.85
	0°C	3	0.59	9	0.69	11	0.79	12	0.99
$x_2 = 0.35$	RT	2.8	0.15	3	0.16	8	0.17	10	0.19
	0°C	9	0.22	15	0.25	18	0.27	22	0.50

Table 1.
Depth (h) and width (w) of the lines in the Ga^+ FIB written open-square patterns in a-$Si_{1-x}C_x$:H [32].

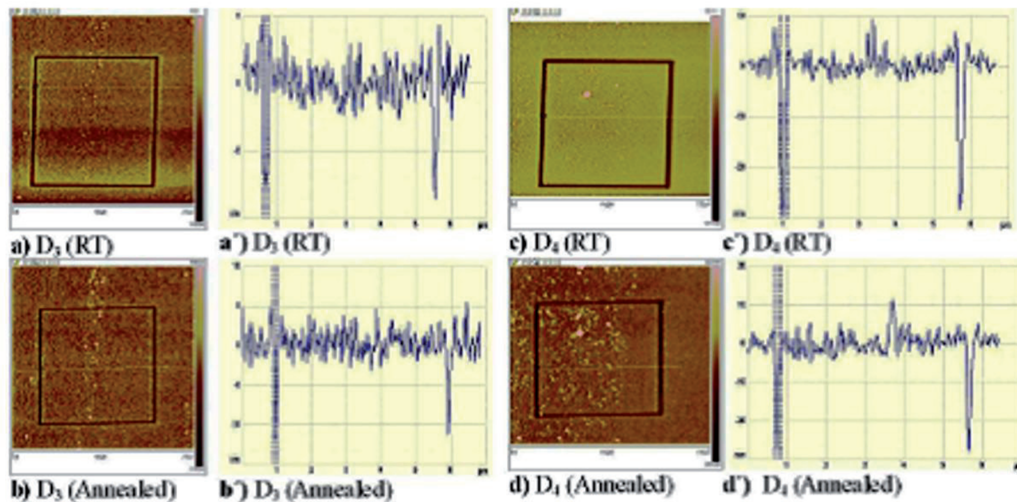

Figure 13.
A set of AFM topographic images of Ga^+ FIB-patterned open-square patterns in a-$Si_{1-x}C_x$:H (x = 0.35) samples: Implanted at a dose D_3 = 2.5 × 10^{16} cm^{-2}, before (a) and after annealing (b), and implanted at a dose D_4 = 1.25 × 10^{17} cm^{-2}, before (c) and after annealing (d); also shown are their corresponding cross-sections (a', b', c' and d') [32].

nonirradiated film areas. This effect is expected to be overridden though by the reduced absorption in the irradiated areas, as a result of thermal annealing of the ion irradiation-induced defects, similarly to the Ga^+ broad-beam implanted case [30].

As demonstrated, the AFM analysis of the Ga^+ FIB-implanted a-$Si_{1-x}C_x$:H samples at RT and at 0°C has revealed an increase of both the depth and the width of the individual lines within the FIB written patterns at lower temperature. This is presumably due to an increased ion beam-induced sputtering yield, in good agreement with the previous results for the case of Ga^+ broad-beam implantation in a-$Si_{1-x}C_x$:H, presented in a previous chapter section. Hence, the present results again suggest that the preferable conditions for optical data storage for archival storage

uses would be choosing Ga^+ FIB implantation in a-SiC:H films with an optimal dose at room temperatures. The AFM data also confirm that no advantage would be gained by applying post-implantation annealing treatments.

5. Conclusions

- The present study has shown the existence of optimal conditions for Ga ion implantation of a-SiC:H films in order to achieve large ion beam-induced optical contrast with less topographic change. Low ion irradiation doses are not only sufficient but also preferable for achieving strong modification of the optical absorption, which is required for applications in optical data storage and for creating permanent optical archives.

- With view of optimizing the FIB optical patterning of a-SiC:H, studying the effects of the implantation temperature and post-implantation thermal annealing on the Ga^+ broad ion beam-induced optical contrast formation in the implanted films has been undertaken. The expected benefit for the optical data storage method, which relies on achieving reduced optical transmission detected by scanning near-field optical microscopy, was that a lower implantation temperature would result in an increased amount of ion beam-induced defects, leading to an absorption increase, i.e., further decrease in transmission (greater readout contrast). This expected effect was indeed observed but was overridden by an additional effect of increased ion beam-induced sputtering yield, which greatly reduced the film thickness and hence increased the optical transmission.

- The expected effect of the use of higher implantation temperatures, or high-temperature post-implantation annealing, was that there would be an increase in the optical reflectivity and hence decrease in transmission, since there was expected Ga clusters coalescing into bigger light-reflecting Ga colloid particles. This effect of reflectivity increase was indeed observed but was overridden by a decrease in absorption (transmission increase) in the high-temperature implanted or annealed samples, due to a decrease in the defect concentration as a result of self-annealing.

- In the case of the Ga^+-focused ion beam writing of optical patterns in a-SiC:H films, an increase of both the depth and the width of the individual lines within the FIB written patterns at the lower implantation temperatures, as a result of an increased ion beam-induced sputtering, has been observed. These results are also in good agreement with the previous data for the broad-beam implantation case.

- The AFM results for the RT implanted and the thermally annealed samples revealed slight changes in the depth of the individual lines within the FIB written patterns. The noticeable decrease of the depth of the individual lines after the thermal annealing, and hence obtained slight thickness increase in the irradiated areas of the films, which should contribute to an increased optical absorption thereof, and hence should result in an increased optical contrast as compared to the nonirradiated film areas, is overridden by the reduced absorption in the irradiated areas, as a result of the thermal annealing of the irradiation-induced defects, in agreement with the results for the broad-beam implantation case.

- The AFM analysis of the Ga^+ FIB-patterned a-$Si_{1-x}C_x$:H samples at RT and at 0°C showed an increase of both the depth and the width of the individual lines within the written patterns at the lower temperature case, due to an increased ion beam-induced sputtering. This data is in good agreement with previous results for the case of Ga^+ broad-beam implantation and again suggests that the preferable conditions for the optical data storage method would be using gallium ion implantation in amorphous silicon carbide films at room temperatures with an optimal gallium ion dose. Similarly, the AFM data also confirm that no advantage is expected to result from further post-implantation annealing treatments.

- In conclusion, we can assume that the best conditions for optical data storage for archival storage applications, when using Ga^+ ion implantation in a-SiC:H films, would be employing an optimal gallium ion dose at room temperatures. The fact that the optimum implantation temperature for optical data storage applications appears to be that of room temperature is fortuitous since the implications are that the required ion-implantation processing could be simplified and reduced in cost.

Acknowledgements

Throughout this work, the support of the Bulgarian Academy of Sciences and Maria Curie-Sklodowska University in Lublin, Poland, has been invaluable. Also gratefully acknowledged is the help of the staff of the Ion Beam Centre at the Helmholtz-Zentrum Dresden-Rossendorf e.V., Germany, for performing the focused ion beam implantation.

Author details

Tania Tsvetkova
Institute of Solid State Physics, Bulgarian Academy of Sciences, Sofia, Bulgaria

*Address all correspondence to: tsvet@issp.bas.bg

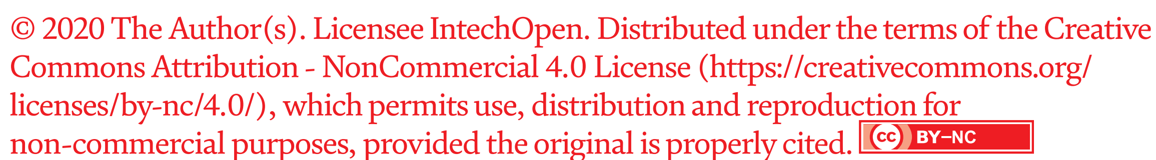

IntechOpen

© 2020 The Author(s). Licensee IntechOpen. Distributed under the terms of the Creative Commons Attribution - NonCommercial 4.0 License (https://creativecommons.org/licenses/by-nc/4.0/), which permits use, distribution and reproduction for non-commercial purposes, provided the original is properly cited.

References

[1] Enterprise Strategy Group (ESG) Research Report. Digital Archiving: End-User Survey & Market Forecast; 2006-2010

[2] Enterprise Strategy Group (ESG) Archive Multi-Client Study; September 2006

[3] Powell JA, Matus L. In: Harris GL, Yang CYW, editors. Amorphous and Crystalline Silicon Carbide. Berlin: Springer; 1989

[4] Kanicki J. Amorphous and Microcrystalline Semiconductor Devices. Boston, London: Artech House; 1991

[5] Tsvetkova T, Tzenov N, Tzolov M, Dimova-Malinovska D, Adriaenssens GJ, Pattyn H. Optical properties and chemical structure of ion implanted a-SiC:H. Vacuum. 2001;**63**:749

[6] Bischoff L, Teichert J, Kitova S, Tsvetkova T. Optical pattern formation in a-SiC:H films by Ga^{+} ion implantation. Vacuum. 2003;**69**:73

[7] Tsvetkova T, Angelov O, Sendova-Vassileva M, Dimova-Malinovska D, Bischoff L, Adriaenssens GJ, et al. Structural and optical properties modification of a-SiC:H by Ga^{+} ion implantation. Vacuum. 2003;**70**:467

[8] Tsvetkova T, Takahashi S, Zayats A, Dawson P, Turner R, Bischoff L, et al. Near-field optical mapping of ion-implanted patterns fabricated in amorphous silicon carbide. Vacuum. 2005;**79**:94-99

[9] Tsvetkova T, Takahashi S, Zayats A, Dawson P, Turner R, Bischoff L, et al. Fabrication of nano-scale optical patterns in amorphous silicon carbide with focused ion beam writing. Vacuum. 2005;**79**:100-105

[10] Kalbitzer S. Semiconductors for optical memories. Current Opinion in Solid State & Materials Science. 2002;**6**:271

[11] Müller G. The contribution of ion-beam techniques to the physics and technology of amorphous semiconductors. Nuclear Instruments and Methods in Physics Research Section B. 1993;**957**:80-81

[12] Hirvonen JK. Ion Implantation and Ion Beam Processing of Materials. Amsterdam, North Holland; 1984

[13] Böhringer K, Jousten K, Kalbitzer S. Development of a high-brightness gas field-ionization source. Nuclear Instruments and Methods in Physics Research Section B. 1988;**30**:289

[14] Ruttensberger B, Krotz G, Muller G, Derst G, Kalbitzer S. Crystalline-amorphous contrast formation in thermally crystallized SiC. Journal of Non-Crystalline Solids. 1991;**137-138**:635

[15] Richards D, Zayats AV, editors. Nano-optics and near-field microscopy. Philosophical Transactions of the Royal Society. 2004;**362**:699-812

[16] Ocelic N, Hillenbrand R. Subwavelength-scale tailoring of surface phonon polaritons by focused ion-beam implantation. Nature Materials. 2004;**3**:606

[17] Birukawa M, Ito E, Narumi K, Kojima R, Yamada N, Mizukuki T, Nakaoki A, et al. Rewritable dual-layer recording with near-field coupled SIL system. Proc. of EPCOS. 2008. Prague; 2008. Available from: www.epcos.org

[18] Liu Q, Fukaya T, Cao S, Guo C, Zhang Z, et al. Study on readout durability of super-RENS disk. Optics Express. 2008;**16**:213

[19] Tzenov N, Dimova-Malinovska D, Marinova T, Krastev V, Tsvetkova T. X-ray

photoelectron study of Sn^+ implanted a-$Si_{1-x}C_x$:H thin films. Materials Science and Engineering B. 1995;**29**:165

[20] Tzenov N, Dimova-Malinovska D, Marinova T, Krastev V, Tsvetkova T. Modification of magnetron sputtered a-$Si_{1-x}C_x$:H films by implantation of Ge^+. Nuclear Instruments and Methods in Physics Research Section B. 1996;**112**:342

[21] Tzenov N, Dimova-Malinovska D, Tsvetkova T. Modification of magnetron sputtered a-$Si_{1-x}C_x$:H films by implantation of Sn^+. Materials Research Society Symposium Proceedings. 1996;**396**:243

[22] Tsvetkova T. Ion beam modification of amorphous silicon-carbon alloys. In: Singh J, Copley S, Mazumder J, editors. Beam Processing of Advanced Materials. Metals Park: ASM International; 1996. p. 321

[23] Mohr W, Tsai C, Street R. Properties and local structure of plasma-deposited amorphous silicon-carbon alloys. Materials Research Society Symposium Proceedings. 1986;**70**:319

[24] Herremans H, Grevendonk W, van Swaaij RACMM, van Sark WGJHM, Berntsen AJM, Arnold Bik WM, et al. Structural, compositional and optical properties of hydrogenated amorphous silicon-carbon alloys. Philosophical Magazine B. 1992;**66**:787

[25] Hole DE, Townsend PD, Barton JD, Nistor LC, Landuyt J. Gallium colloid formation during ion implantation of glass. Journal of Non-Crystalline Solids. 1995;**180**:266-274

[26] Takahashi S, Dickson W, Pollard R, Zayats AV. Near-field magneto-optical analysis in reflection mode SNOM. Ultramicroscopy. 2004;**100**:443

[27] Karrai K, Grober RD. Piezoelectric tip-sample distance control from near field optical microscopes. Applied Physics Letters. 1995;**66**:1842

[28] Hoffmann P, Dutoit B, Salathe RP. Comparison of mechanically drawn and protection layer chemically etched optical fiber tips. Ultramicroscopy. 1995;**61**:165

[29] Pangaribuan T, Yamada K, Jiang SD, Ohsawa H, Ohtsu M. Reproducible fabrication technique of nanometric tip diameter fiber probe for photon scanning tunneling microscope. Japanese Journal of Applied Physics. 1992;**31**:L1302

[30] Tsvetkova T, Wright CD, Kitova S, Bischoff L, Zuk J. Effects of implantation temperature and thermal annealing on the Ga^+ ion beam induced optical contrast formation in a-SiC:H. Nuclear Instruments and Methods in Physics Research Section B. 2013;**307**:71

[31] Tsvetkova T, Wright CD, Craciun MF, Bischoff L, Angelov O, Dimova-Malinovska D. Thermal effects on the Ga^+ ion beam induced structural modification of a-SiC:H. Journal of Physics Conference Series. 2012;**398**:012048

[32] Tsvetkova T, Wright CD, Hosseini P, Bischoff L, Zuk J. Implantation temperature effects on the nanoscale optical pattern fabrication in a-SiC:H. Acta Physica Polonica A. 2013;**123**:952